Available online at www.sciencedirect.com
ScienceDirect
Journal of the European Ceramic Society 27 (2007) 3941–3945
www.elsevier.com/locate/jeurceramsoc

# Processing and phase separation of LSMO-based multiferroic composite ceramics

G.B. Song [a,b,*], J.S. Amaral [c], V.S. Amaral [c], A.L. Kholkin [a]

[a] Department of Ceramics and Glass Engineering/CICECO, University of Aveiro, 3810-193 Aveiro, Portugal
[b] School of Material Science and Engineering, Southwest University of Science and Technology, Mianyang 621002, PR China
[c] Department of Physics, University of Aveiro/CICECO, 3810-193 Aveiro, Portugal

Available online 26 March 2007

**Abstract**

In this paper, the effect of processing conditions on phase separation and crystal structure of $(x)$ $La_{0.625}Sr_{0.375}MnO_3$–$(1-x)$ $LuMnO_3$ composite system was studied by XRD and SEM. The results confirm that there is a solid solution of monoclinic phase of space group $P112_1/a$ in this system, i.e. $(La_{0.625}Sr_{0.375})_x$ $Lu_{1-x}MnO_3$ is formed for $x = 0.980$–$1.0$. For $0 < x \leq 0.975$, the immiscibility region shows clear separation of both La-rich and Lu-rich phases. The optimal preparation conditions were found for this system: sintering at 1250 and 1350 °C for samples of monoclinic La-rich phase and for the immiscibility region, respectively.


*Keywords:* Manganites; Composites

## 1. Introduction

The term multiferroics has been used[1,2] to describe materials in which two or all three phenomena: ferroelectricity, ferromagnetism (FM), and ferroelasticity occur in the same phase or in the multiphase composite. This means that they have a spontaneous magnetization that can be changed by an applied electric field, a spontaneous electrical polarization that can be modified by an applied magnetic field,[3] or a spontaneous deformation that can be reoriented electrically and/or magnetically. The coupling between ferroelectricity and ferroelasticity is well established, and leads to the wide use of ferroelectric materials in transducer applications.[2] Similarly, the coupling between ferromagnetism and ferroelectricity results in magnetoelectric/piezomagnetic effects and the consequent application of piezomagnets as magnetomechanical actuators. Since the first multiferroic material was discovered,[4] many compounds were found to have multiferroic properites, such as $Cr_2O_3$,[5] $Ti_2O_3$,[6] $GaFeO_3$,[7] boracites,[4] phosphates,[8] $PbFe_{0.5}Nb_{0.5}O_3$.[9] In the past few years, there has been renewed interest in studying the perovskite-based multiferroic materials, such as rare earth manganates $TbMn_2O_5$,[10] $YMnO_3$, or $BiMnO_3$,[11] which have higher Curie temperatures and larger magnetoelectric effects. Furthermore, current efforts have been made to synthesize the new multiferroic in the form of thin films, by employing ferroelectric and magnetic compounds to make a nanocomposite or a superlattice/multilayer structure.[12–14] Among them, many researchers are focusing on the structure and properties of various rare earth perovskite manganites ($REMnO_3$). The $(x)$ $La_{0.625}Sr_{0.375}MnO_3$ (LSMO)–$(1-x)$ $LuMnO_3$ (LMO) system is one of the interesting examples of multiferroic composites. Huang et al.[15,16] studied abnormal lattice effect on the phase diagram, magnetic transport and charge ordering induced by phase separation in polycrystalline $La_{0.7-x}Lu_xSr_{0.3}MnO_3$ perovskites. Park et al.[17] observed percolative conduction in (La, Lu, Sr)$MnO_3$ and discovered that an almost complete chemical immiscibility exists between FM-metallic (M) LSMO and FE-insulating (I) LMO. The solubility of LMO in LSMO was found to be about 1% by monitoring $T_C$ for each mixture. However, the detailed X-ray study of solid solubility in $(1-x)$ LSMO–$x$ LMO system at small $x$ is still missing. The exact solubility limit of LMO into LSMO is still under debate. There are not enough evidence to confirm that there exists a coupling between ferromagnetic and ferroelectric phases. This paper is devoted to the fabrication and structural investigation of $(x)$ LSMO–$(1-x)$ LMO multiferroic ceramics in the full range of compositions, focusing on solid solution region.

* Corresponding author.
*E-mail address:* gbsong@cv.ua.pt (G.B. Song).

0955-2219/$ – see front matter © 2007 Elsevier Ltd. All rights reserved.
doi:10.1016/j.jeurceramsoc.2007.02.071

## 2. Experiment

In this study, all samples of $(x)$ $La_{0.625}Sr_{0.375}MnO_3$–$(1-x)$ $LuMnO_3$ system ($x = 1.0$, 0.995, 0.990, 0.985, 0.980, 0.975, 0.9, 0.8, 0.7, 0.6, 0.5, 0.4, 0.3, 0.25, 0.2, 0.1 and 0.0) were prepared by solid-state chemical reaction. The purity of all starting materials ($La_2O_3$, $Lu_2O_3$, $SrCO_3$, and $Mn_2O_3$) was 99.99%. Their particle sizes were measured by Laser Particle Analyzer (Mast Sizer 2000). The particle sizes of $La_2O_3$, $Lu_2O_3$, $SrCO_3$, and $Mn_2O_3$ are 4–10, 4–10, 2–6 and 4–9 μm, respectively. The raw powders with proper compositions were weighed, thoroughly mixed and ground in an agate mortar, and then calcined in air at 900 °C for about 12 h. After regrinding and remixing the calcined powders were isostatically pressed into the disks with a diameter of 10 mm and thickness of 1–2 mm. The pellets were then sintered at 1250–1300 °C for 24 h in air, and then cooled in the furnace to room temperature. The above process was repeated several times until the homogeneity of the samples was reached as tested by X-ray diffraction.

X-ray diffraction data were collected by a Rigaku D/max-RC rotating target X-ray diffractometer (30mA × 40 kV). The Cu Kα radiation and a graphite monochromator were used. The data for the determination of the crystal structure and accurate lattice parameters of the $(La_{0.625}Sr_{0.375})_x$ $Lu_{(1-x)}$ $MnO_3$ samples were collected in a step scan mode with scanning steps of $2\theta = 0.02°$ and a sampling time of 6 s.

The morphology and composition of ceramics grains was charactered by scanning electronic microscopy (SEM) (Hitachi, S-4100) coupled with energy dispersive analysis.

## 3. Results and discussion

### 3.1. Processing method

#### 3.1.1. Sintering temperatures

Based on earlier investigations[15–18] the sintering temperature for (La, Sr, Lu)$MnO_3$ ceramics was reported to be in the range 1200–1400 °C. We attempted to process our samples of $(x)$ $La_{0.625}Sr_{0.375}MnO_3$–$(1-x)$ $LuMnO_3$ system at two temperatures: 1250 and 1350 °C. It was found that the temperature of 1350 °C is suitable for samples of Lu-rich compositions. When the samples of La-rich were prepared under 1350 °C, it was very difficult to get single phase sample of $La_{0.625}Sr_{0.375}MnO_3$ composition. Our results confirmed that there are at least monoclinic La-rich phase, and manganese oxides in this sample. Further experiments confirmed that the temperature of 1250 °C is suitable for samples of La-rich composition. But they were still needed to be sintered several times under this temperature.

#### 3.1.2. Sintering steps

It was difficult to get high-quality samples using one step calcination and sintering procedure at both temperatures (1250 or 1350 °C). One can see from Fig. 1a that there are always manganese oxide phases ($Mn_3O_4$) in addition to monoclinic phase of La-rich compositions ($x = 1.0$) for the multiple processing steps ($N = 1$–3) at 1250 °C. The content of $Mn_3O_4$ phase decreases with increasing number of calcination steps. It is also seen that no obvious $Mn_3O_4$ phase presence is observed in the sample calcined four times. It has to be concluded that multiple calcination step ($N > 3$) is prerequisite for the sintering of high-quality (La, Sr, Lu)$MnO_3$ ceramics.

From Fig. 1b one can see that there are just La-rich monoclinic phase and Lu-rich hexagonal phase in the sample for $x = 0.5$ calcined four times and sintered at 1350 °C. But many reflections (marked by circles) cannot be indexed with La-rich monoclinic phase and Lu-rich hexagonal phase in the sample for $x = 0.5$ processed with 2 steps. The SEM images show that there are three types of grains in the sample for $x = 0.5$ sintered two times (Fig. 2a ), and only two types of grains in the sample with four sintering steps (Fig. 2b). The SEM result of sample with $x = 0.5$ (four sintering steps) is consistent with that of XRD (Fig. 1b). The results of EDS analysis confirmed that the composition of "a" particle is Lu-rich, that of "b" particle is La-rich, with "c" being between "a" and "b", the La:Lu:Sr:Mn compositions of "a", "b" and "c" particles are 0.67:46.94:4.20:48.18, 36.15:3.31:10.99:49.55 and 28.43:8.99:4.82:57.77, respectively. All the results of XRD, SEM and EDS analysis confirm that repeated milling and calcination is necessary for the processing of (La, Sr, Lu)$MnO_3$ system.

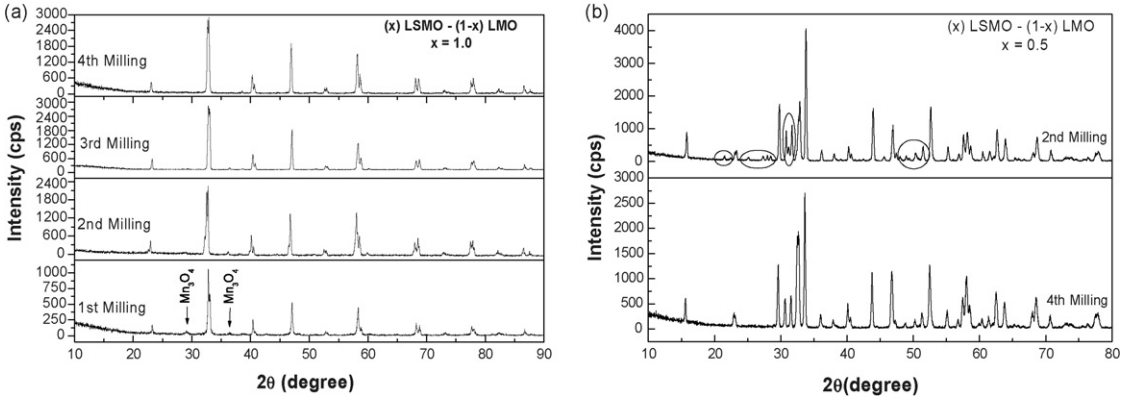


Fig. 1. XRD patterns of samples subjected to different number sintering steps in $(x)$ LSMO–$(1-x)$ LMO system (a) $x = 1.0$ at 1250 °C, and (b) $x = 0.5$ at 1350 °C.

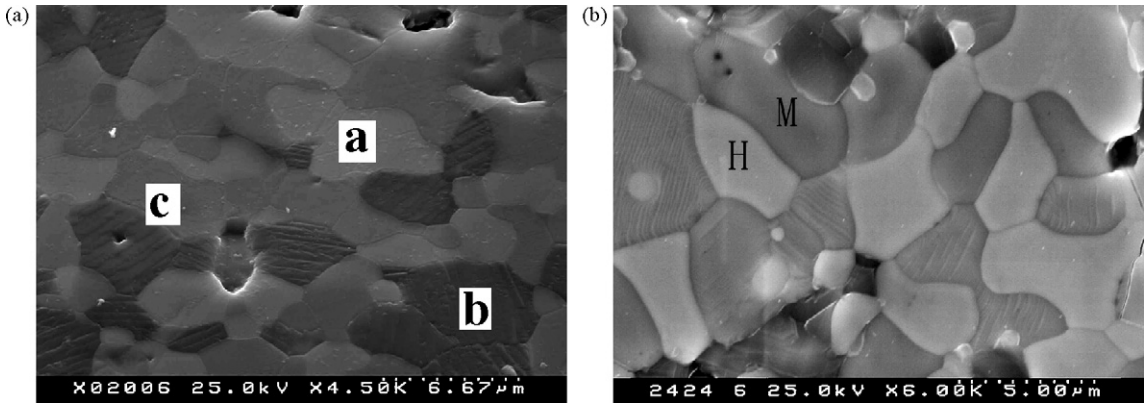


Fig. 2. SEM images of composite sample ($x = 0.5$) processed with different number of milling/sintering steps: (a) $N = 2$, (b) $N = 4$.

### 3.1.3. Effect of sintering atmosphere

Several literature reports indicated that $La_{0.625}Sr_{0.375}MnO_3$ ceramics belong to the rhombohedral phase.[15–18] Few papers reported the existence of the monoclinic phase.[19] We studied the effect of ambient atmosphere on the crystallographic structure of the samples of La-rich compositons. Fig. 3 is the XRD pattern of sample for $x = 0.985$ in ($x$) LSMO–($1 - x$) LMO system under different calcination atmosphere. One can see that all of XRD reflections of sample for $x = 0.985$ sintered in oxygen can be indexed with rhombohedral structure, $R\bar{3}C$ space group (PDF number: 50–308). Compared with the XRD results of sample for $x = 0.985$ sintered in oxygen, the XRD results of sample for $x = 0.985$ sintered in air is obviously different. The peaks of $2\theta$ around 32.94°, 40.44°, 53.06°, 58.48°, and 78.24° split into two peaks. And all of XRD peaks of sample for $x = 0.985$ sintered in air can be indexed with monoclinic structure, space group *P2/c* (PDF number: 40–1100). This result indicates that the calcinations atmosphere plays important role in the formation of the structure of La-rich samples. It is evident that there are more oxygen vacancies in samples calcined in air, as compared to those processed in oxygen. This may result in deviation of structural symmetry from rhombohedral to monoclinic one. Huang et al.[19] discussed similar structural order in undoped lanthanum manganite. It is thus necessary to study this effect in a more detail in future.

### 3.2. The phase separation of ($x$) LSMO–($1 - x$) LMO system

Some results about related system have been already published.[15–18] Rhombohedral (R) La-rich and hexagonal (H) Lu-rich phases were found. Huang et al.[19] also found a monoclinic phase of space group $P112_1/a$ and an orthorhombic phase of space group *Pnma*. Park et al.[17] demonstrated chemical phase separation in this system. They found that the sintered composites show both rhombohedral and hexagonal diffraction patterns. They thought that the solubility of $LuMnO_3$ into $La_{0.625}Sr_{0.375}MnO_3$ is about 1%. Our current results show that there are both monoclinic La-rich and hexagonal (H) Lu-rich phases present under our sintering conditions. The XRD patterns of samples of ($x$) LSMO–($1 - x$) LMO system are shown in Fig. 4. From this figure, one can see that there is a single phase,

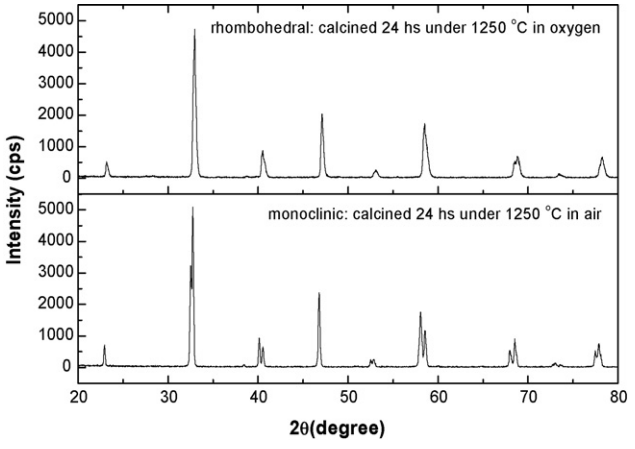


Fig. 3. XRD patterns of samples for $x = 0.985$ processed in different atmospheres.

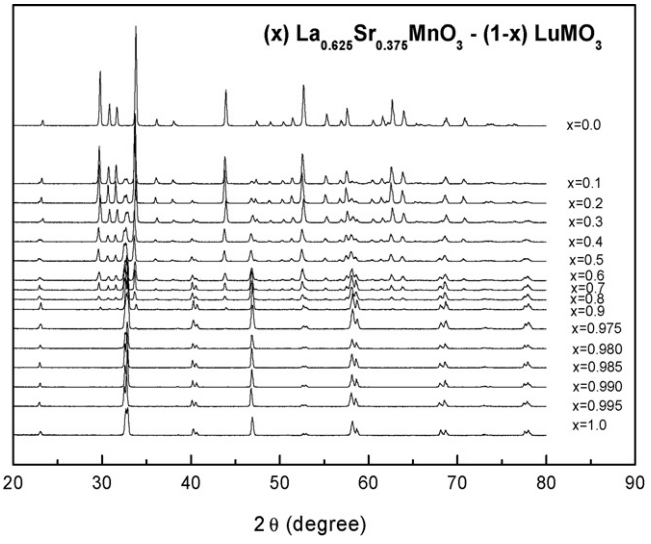


Fig. 4. XRD patterns of ($x$) LSMO–($1 - x$) LMO composite samples ($x = 0$–1).

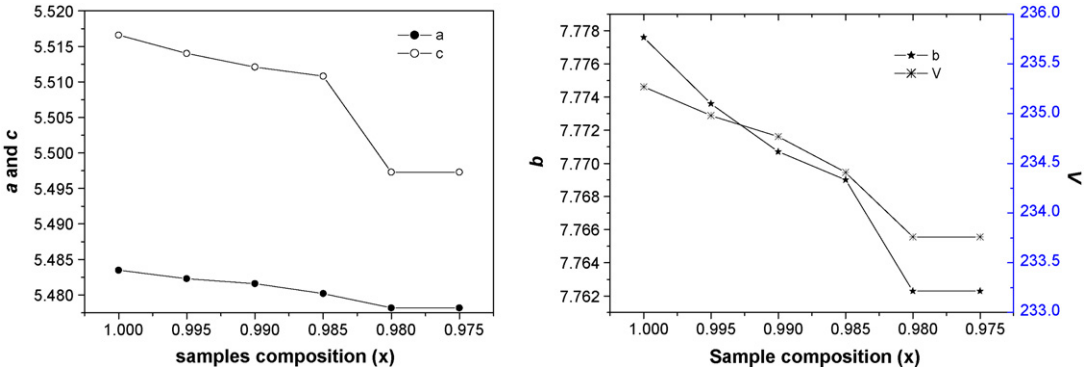


Fig. 5. Variation of lattice parameters $a$, $b$, $c$ (Å) and $V$ (Å$^3$) with composition ($x$) of La-rich samples of monoclinic phase.

a monoclinic phase of space group $P112_1/a$ with $x = 0.980$–$1.00$. There are both monoclinic La-rich and hexagonal (H) Lu-rich phases with $0 < x \leq 0.975$. With increasing $LuMnO_3$ content, the intensity of monoclinic La-rich peaks decreases gradually while the intensity of hexagonal (H) Lu-rich phase distinctly increases. According to above results, the solid solution of ($x$) LSMO–($1 - x$) LMO system is formed at $x = 0.98$–$1.0$, i.e. the solubility of $LuMnO_3$ into $La_{0.625}Sr_{0.375}MnO_3$ is about 2% in our case.

Furthermore, phase separation is also confirmed by SEM analysis. Fig. 2b shows the morphology of the sample with $x = 0.5$. From this figure, one can see that there are two types of grains in this sample differing in the contrast: one is more bright than the other (dielectric phase). EDS analysis results also confirm that the bright grains are hexagonal phase of Lu-rich and the while others are of monoclinic phase of La-rich composition. These results are consistent with our XRD study.

### *3.3. Crystal structure of solid solution of (x) LSMO–(1 − x) LMO system*

The crystal structures were refined by the Rietveld method using the DBWS-9411 program.[20,21] The starting model for the structure refinements of the ($x$) LSMO–($1 - x$) LMO samples ($x = 1.0$, 0.995, 0.990, 0.985, 0.980, 0.975) was taken from Ref.19 Table 1 and Fig. 5 present the lattice parameters of monoclinic phase of solid solution samples. With increasing Lu content in samples, the lattice parameters were decreased gradually. These results confirmed that the solubility of $LuMnO_3$ into $La_{0.625}Sr_{0.375}MnO_3$ is about 2%.

Table 1
Lattice parameters of solid solution of $(La_{0.625}Sr_{0.375})_x\ Lu_{1-x}\ MnO_3$ in monoclinic phase

| $x$ | $a$ | $b$ | $c$ | $\beta$ | $V$ | $R_{wp}$ |
|---|---|---|---|---|---|---|
| 1 | 5.4835 | 7.7776 | 5.5166 | 90.5018 | 235.27 | 9.89 |
| 0.995 | 5.4823 | 7.7736 | 5.514 | 90.6266 | 234.98 | 8.65 |
| 0.99 | 5.4816 | 7.7707 | 5.5121 | 90.7132 | 234.77 | 8.90 |
| 0.985 | 5.4802 | 7.7690 | 5.5108 | 90.5745 | 234.41 | 9.52 |
| 0.98 | 5.4782 | 7.7623 | 5.4973 | 90.4713 | 233.76 | 8.32 |
| 0.975 | 5.4782 | 7.7623 | 5.4973 | 90.4713 | 233.76 | 9.35 |

## 4. Conclusion

The effect of sintering conditions on phase separation and crystal structure of ($x$) LSMO–($1 - x$) LMO system was studied by XRD and SEM. The optimal preparation conditions for this system were 1250 and 1350 °C for samples of monoclinic La-rich phase and for the immiscibility region, respectively. The third (transient) phase in the demixing region was eliminated by using at least 4 calcination steps. There is a solid solution of monoclinic phase in the system $(La_{0.625}Sr_{0.375})_x\ Lu_{1-x}MnO_3$ with $x = 0.980$–$1.0$. In the immiscibility region, clear separation of both La-rich phase and Lu-rich phases occurs for $0 < x \leq 0.975$.

## Acknowledgements

G.B. Song acknowledges FCT (Portugal) for financial support through post-doctoral grant (SFRH/BPD/20557/2004). The work is conducted within STREP "Multiceral" funded by EU (NMP-CT-2006-032616). Mr. Zhi Fu is acknowledged for help with dielectric measurements.

## References

1. Schmid, H., Multi-ferroic magnetoelectrics. *Ferroelectrics*, 1994, **162**, 317–338.
2. Hill, N. A., Density functional studies of multiferroic magnetoelectrics. *Annu. Rev. Mater. Res.*, 2002, **32**, 1–37.
3. Fiebig, M., Revival of the magnetoelectric effect. *J. Phys. D: Appl. Phys.*, 2005, **38**, R123–R152.
4. Ascher, E., Rieder, H., Schmid, H. and Stossel, H., Some properties of ferromagnetoelectric nickel-iodine boracite $Ni_3B_7O_{13}I$. *J. Appl. Phys.*, 1966, **37**, 1404–1405.
5. Rado, G. T. and Folen, V. J., Observation of the magnetically induced magnetoelectric effect and evidence for antiferromagnetic domains. *Phys. Rev. Lett.*, 1961, **7**, 310–311.
6. Alshin, B. I. and Astrov, D. N., Magnetoelectric effect in titanium oxide $Ti_2O_3$. *Sov. Phys.-JETP*, 1963, **17**, 809–811.
7. Rado, G. T., Observation and possible mechanisms of magnetoelectric effects in a ferromagnet. *Phys. Rev. Lett.*, 1964, **13**, 335–337.
8. Santoro, R. P., Segal, D. J. and Newnham, R. E., Magnetic properties of $LiCoP_4$ and $LiNiPO_4$. *J. Phys. Chem. Solids*, 1966, **27**, 1192–1193.
9. Watanabe, T. and Kohn, K., Magnetoelectric effect and low-temperature transition of $PbFe_{0.5}Nb_{0.5}O_3$ single-crystal. *Phase Trans.*, 1989, **15**, 57–68.
10. Hur, N., Park, S., Sharma, P. A., Ahn, J. S., Guha, S. and Cheong, S.-W., Electric polarization reversal and memory in a multiferroic material induced by magnetic fields. *Nature*, 2004, **429**, 392–395.

11. Huang, Z. J., Cao, Y., Sun, Y. Y., Xue, Y. Y. and Chu, C. W., Coupling between the ferroelectric and antiferromagnetic orders in $YMnO_3$. *Phys. Rev. B*, 1997, **56**, 2623–2626.
12. Nan, C. W., Liu, G. and Lin, Y. H., Influence of interfacial bonding on giant magnetoelectric response of multiferroic laminated composites of $Tb_{1-x}Dy_xFe_2$ and $PbZr_xTi_{1-x}O_3$. *Appl. Phys. Lett.*, 2003, **83**, 4366–4368.
13. Dong, S. X., Li, J. F., Viehland, D, Cheng, J. and Cross, L. E., A strong magnetoelectric voltage gain effect in magnetostrictive-piezoelectric composite. *Appl. Phys. Lett.*, 2004, **85**, 3534–3536.
14. Liu, X. M., Fu, S. Y. and Huang, C. J., Synthesis and magnetic characterization of novel $CoFe_2O_4$-$BiFeO_3$ nanocomposites. *Mater. Sci. Eng. B*, 2005, **121**, 255–260.
15. Huang, Y. H., Luo, F., Li, Y., Wang, Z. M., Liao, C. S. and Yan, C. H., Abnormal lattice effect on magnetic/transport phase diagram in $La_{0.7-x}Lu_xSr_{0.3}MnO_3$ perovskites. *J. Appl. Phys.*, 2002, **91**, 10218–10220.
16. Song, W., Luo, F., Huang, Y. H., Yan, C. H., Sun, B. Z. and He, L. L., Charge ordering induced by phase separation in polycrystalline $La_{0.7-x}LuxSr_{0.3}MnO_3$ perovskites. *J. Appl. Phys.*, 2004, **96**, 2731–2735.
17. Park, S., Hur, N., Guha, S. and Cheong, S.-W., Percolative conduction in the half-metallic-ferromagnetic and ferroelectric mixture of $(La,Lu,Sr)MnO_3$. *Phys. Rev. Lett.*, 2004, **92**, 167–206.
18. Sun, B. Z., He, L. L., Luo, T. F. and Yan, C. H., Effects of A-site doping on microstructure and phase separation of $La_{0.5}RE_{0.2}Sr_{0.3}MnO_3$ (RE = Eu, Ho, Yb, Lu). *Mater. Lett.*, 2005, **59**, 1507–1510.
19. Huang, Q., Santoro, A., Lynn, J. W., Erwin, R. W., Borchers, J. A., Peng, J. L. *et al.*, Structure and magnetic order in undoped lanthanum manganite. *Phys. Rev. B*, 1997, **55**, 14987–14999.
20. Rietveld, H. M., Line profiles of neutron powder-diffraction peaks for structure refinement. *Acta Crystallogr.*, 1967, **229**, 151–152.
21. Young, R. A., Sakthivel, A., Moss, T. S. and Paiva-Santos, C. O., DBWS-9411—an upgrade of the DBWS*.* programs for Rietveld re-finement with PC and mainframe computers. *J. Appl. Crystallogr.*, 1995, **28**, 336–367.